Pharmacophore Modeling, Docking, and Molecular Dynamics Simulation of Flavonoids as Inhibitors of Urokinase-type Plasminogen Activator

Bina Lohita Sari[1,2], Slamet Ibrahim[1] & Daryono Hadi Tjahjono[1]*

[1]School of Pharmacy, Institut Teknologi Bandung, Jalan Ganesha 10, Bandung 40132, Indonesia
[2]Pharmacy Study Program, Pakuan University, Jalan Pakuan PO BOX 452, Bogor 16143, Indonesia
*E-mail: daryonohadi@fa.itb.ac.id

Abstract. The urokinase-type plasminogen activator (uPA) system plays a significant role in the invasion and metastasis of cancer cells. The present study was conducted to investigate natural product compounds as inhibitors and hit molecules of uPA using in-silico analysis. A pharmacophore model was built to screen the Indonesian Herbal Database (HerbalDB) to obtain inhibitors of different scaffolds. Based on the molecular docking score, four ligands were selected as potential uPA inhibitors. Subsequently, the stability of the ligand-uPA complex was analyzed using molecular dynamics (MD) simulation. An RMSD graph of the backbone protein and the RMSF values of the amino acid residues were also determined. In addition, the MM-PBSA method was applied to calculate the free binding energy. According to the results, Model_3, characterized by aromatic rings 23 (F1 and F2), cationic H-bond donor (F3), and metal ligator (F4) features, had an adequate goodness-of-hit score (GH). The four top-ranked ligands, isorhamnetin, rhamnetin, quercetin, and kaempferol, showed higher docking scores compared to the others. This study confirmed that isorhamnetin, rhamnetin, and kaempferol build stable complexes with uPA with lower binding energy than quercetin.

Keywords: *anti-cancer; flavonoids; in-silico study; isorhamnetin; kaempferol; quercetin; rhamnetin.*

1 Introduction

Urokinase-type plasminogen activator (uPA) belongs to the serine protease class of enzymes, which play a significant role in the regulation of physiological and pathological processes. Furthermore, uPA cleaves the proenzyme/zymogen plasminogen to form active enzyme plasmin and degrades the extracellular matrix (ECM) as well as the basement membranes, directly or indirectly, by activating pro matrix metalloproteinases (pro-MMPs) and promoting cancer cell metastasis as well as invasion [1,2]. uPA is constructed by a C-terminal (≈ 30-kDa) serine

Received September 6th, 2021, Revised November 30th, 2021, Accepted for publication December 10th, 2021
 ISSN: 2337-5760, DOI: 10.5614/j.math.fund.sci.2021.53.3.8

protease domain (SPD) and an N-terminal (≈25-kDa) A-chain, which consist of a growth factor domain and a kringle domain. From the Serin Protease Domain (SPD) of uPA, the active site of Ser-195 is replaced by residues of Ala, namely Lys71, Arg78, Lys82, Lys90, Arg120, and Lys124 [3].

In cancer treatment, a selective inhibitor of uPA can have therapeutic value [2]. Para-substituted benzamidine derivatives, 4-chloro- and 4-trifluoro-methyl-phenylguanidines (Figure 1) as well as amiloride have been recognized as potential uPA inhibitors, albeit of low potency [4].

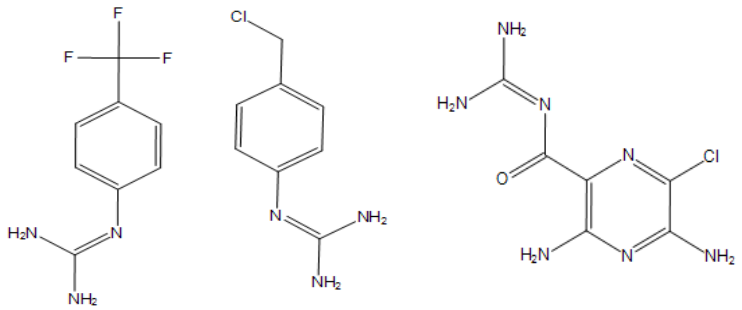

(a) (b) (c)

Figure 1 The structure of previous compounds as uPA inhibitors: 4-trifluoro-methyl-phenylguanidines (a), and 4-chloro-methylphenyl-guanidine (b), amiloride (c).

With considerable progress in the field of cancer therapy, synthetic medicines have become more prevalent, despite the relatively fewer side effects and minimal toxicity of natural compounds [5]. In chemoprevention, natural compounds provide the benefits of safety, efficacy, ready availability, affordability as well as the potential to overcome resistance to other traditional therapies and anticancer drugs [6]. Natural flavonoids with hydroxyl functional groups and O-glycosylation have been even reported for several different properties, including antioxidant, antitumor, influenza virus neuraminidase inhibition, aldehyde oxidase inhibition, immunomodulatory as well as antitubercular activities [7].

In drug development, computer-aided drug design is applied to develop simulation and calculation models. The method used in drug design is either structure-based or ligand-based to facilitate the determination of drug candidates. In this study, the pharmacophore model was used to screen the HerbalDB medicinal plant database, which comprises of 1412 ligands (Biomedical Computation and Drug Design Laboratory, Universitas Indonesia)

[8]. The selected ligands were docked into the binding pocket of uPA by employing the Molecular Operating Environment (MOE) software. In addition, the Protein-Ligand Interaction Profiler (PLIP) web service (https://projects.biotec.tu-dresden.de/plip-web/plip) was applied to visualize the molecular interaction between the flavonoids and the amino acid residues of uPA [9]. Doxorubicin, a known uPA inhibitor, was used as the standard. As the first clinically used anthracycline, doxorubicin is derived from pigment of the *Streptomyces peucetius* bacterium. This natural compound is used to treat cancers of various types of tissue [10]. Doxorubicin is associated with regulating tumor cell survival and apoptosis with TF/FVIIa expression. This complex transforms FX into the serine protease FXa. Besides the proteases FVIIa and FXa, other proteases, such as plasmin, uPA, and tPA, also mediate tissue remodeling [11].

In the present research, Groningen MAchine for Chemical Simulation (GROMACS), a molecular simulation method that uses the messaging passing interface (MPI), was applied to obtain the final accurate receptor-ligand complex [12]. The best two ligands in terms of docking score were further evaluated using MD simulation. In evaluating the simulation, equilibration was monitored and confirmed by examining the stability of the system's temperature, pressure, density, and potential energy as well as the root mean square deviation (RMSD) of the backbone atoms. Subsequently, the binding energies of the two compounds were calculated using MM-PBSA [13].

2 Materials and Methods

2.1 Structure-based Pharmacophore Modeling and Virtual Screening

Several uPA X-ray complexes are documented in the Protein Data Bank (PDB): 1OWD, 1OWE, 1SQO, 1SQT, 1SQA, 1CFL, 1EJN, 1OWH, 1OWK, 1OWJ, 1U6Q, 1YWH, 2OW8, and 1C5X with high resolution [2,14]. PDB ID 1OWE, 1OWH, and 1C5x have resolution < 2Å. PDB ID 1C5X was used to build the pharmacophore model. ESI, a native ligand of 1C5X, features a metal ligator besides an aromatic ring and a donor hydrogen. The native ligand of 4-iodobenzo[β]thiophene-2-carboxamidine (ESI) was preprocessed with hydrogen-added Gasteiger partial charges and energy minimization using the Merck molecular force field 94x (MMFF94x). The MOE Pharmacophore Query Editor was applied to create queries, where six default Ph4 schemes define the annotation of each ligand in the search database (PCH, PCH_All, PPCH, PPCH_All, PCHD, CHD). The structural features in molecules using the Ph4 concept is recognized at the receptor site and thus is responsible for their biological activity [14]. A total of 40 active and 1200 inactive compounds were obtained from Dekois 2.0 as a testing set to validate the pharmacophore model.

The calculated validation parameters, such as total hits (Ht), active hits (Ha), % yield of actives, % ratio of actives, enrichment factor (E), and goodness-of-hit score (GH), were determined to investigate the pharmacophore model [15].

All the compounds from the HerbalDB database were submitted to the Pharmit server (http://pharmit.csb.pitt.edu) for virtual screening of large compound databases using pharmacophores, molecular shapes, and energy minimization [16]. Pharmit uses the Volumetric Aligned Molecular Shapes search method, which uses inclusive and exclusive constraints. Compounds were filtered using Lipinski's rule of five (RO5) by screening for molecular weight < 500, LogP < 5, number of rotating bonds (n-ROTB) < 10, number of H-bond donors < 5, number of H-bond acceptors < 10, PSA < 140, number of aromatic groups < 3 [17]. The enrichment factor (EF) and goodness-of-hit score (GH) values were computed to evaluate the structure-based pharmacophore model score ranges from 0 to 1 (null model to ideal model), which is very good when it is higher than 0.7 [18].

2.2 Molecular Docking

The structure of the 1C5X protein crystal with ESI native ligand in the B chain structure was imported into the MOE 2009.10 software, minimizing the energy and 3D protonating by removing solvent molecules (water). The DUDE dataset, containing 162 active and 9,840 decoy compounds, was used to evaluate the docking method (http://dude.docking.org) [19]. Docking simulation was performed using the placement-scoring parameters while retaining all 10 default poses. Meanwhile, the performance was evaluated by calculating the enrichment factor at 1% as well as the area under the receiver operating characteristics curve (AUC) of each placement-scoring parameter. The maximum attainable value was 100, where AUC = 0.5 conforms to random discrimination between actives and decoys. A value close to 1.0 represents the ideal case, where the known true actives are ranked ahead of the decoys. In addition, Screening Explorer, a web-based interactive application, was used. It supports the scoring functions and aids the selection of active compounds in drug discovery [20]. The best Indonesian natural product compounds were determined based on the Gibbs free energy value (ΔG_{bind}) and molecular interaction with the binding site of uPA.

2.3 Molecular Dynamics (MD) and MM-PBSA Calculation

The protein-ligand complex structure of uPA and the candidate compound was prepared for MD simulation using Gromacs 6.3 software with an AMBER99SB-ILDN forcefield, while the topology and ligand parameters were selected using ACPYPE. Furthermore, the TIP3P water model was selected for solvating complexes. The simulation preparation comprised of a minimization step, 310 K temperature, pressure equilibration, and simulation with a 2fs time step, while the

final MD calculations were performed at 100 ns. The MD simulations were examined based on RMSD as well as RMSF and the binding energies were calculated using MM-PBSA because this has been shown to be an efficient and reliable method to evaluate protein-ligand binding interaction [12, 21]. Hydrogen bond analysis was generated using VMD.

3 Result and Discussion

The 3D structure of a protein with PDB ID 1C5X was used to study the active site of uPA with 4-iodobenzo[β]thiophene-2-carboxamidine (ESI) [20]. A total of 3 hydrogen bonds were discovered between -NH in the amidine ring and Asp189B as well as Gly219B [22].

3.1 Structure-based Pharmacophore Modeling and Virtual Screening

This study used a structure-based pharmacophore model, which relies on information about the target's three-dimensional structure [23]. The active compounds from Dekois 2.0 were benzothiophene, indole, indoline, and quinoline. Figure 1 shows the features of Model_3, where the EF and GH pharmacophore model values were 2.48 and 0.723, respectively, indicating a rational virtual screening. Furthermore, these features represented essential interaction points of the inhibitor binding of uPA: (i) aromatic rings (F1 and F2), which connect to Cys191, Gln192, Ser195, and Trp215; (ii) a cationic H-bond donor (F3) corresponding to Asp189, Ser190, and Gly219; a metal ligator (F4) corresponding to Gly216 (Figure 2). Similarly, a 3D pharmacophore model is suitable for searching for bioactive molecules using virtual screening as well as to support medicinal chemistry in hit expansion and lead optimization [24].

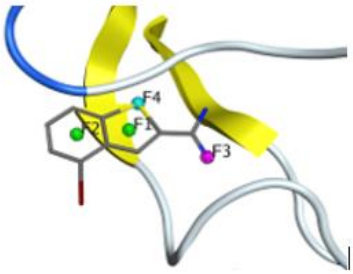

Figure 2 The pharmacophore features of a ligand (encoded as Model_3) in the uPA binding pocket (PDB ID 1C5X). The yellow color indicates the β-sheet in the 3D structure of uPA. F1 and F2 represent the aromatic feature; F3 is the cationic H-bond donor; F4 is the metal ligator.

Subsequently, the Model_3 pharmacophore model was used as a query in screening the HerbalDB database. Molecular shape similarity is an applied method of structure-based virtual screening that is used to filter the number of database compounds [25]. These active sites are represented in the cationic H-bond donor (F3).

3.2 Structure-based Virtual Screening

Screening of the HerbalDB database through the validated pharmacophore model of a uPA inhibitor yielded thirteen hit molecules mapped to Model_3. These compounds were: isorhamnetin, rhamnetin, quercetin, kaempferol, γ-mangosteen, luteolin, baicalein, apigenin, acacetin, lumichrome, formononetin, and scopoletin. These were prepared for molecular docking.

3.3 Molecular Docking

An examination of the lowest RMSD pose showed the MOE's accuracy in reproducing the conformation of small molecules observed in the protein-ligand complex [26]. According to the results, the smallest RMSD value in Alpha Triangle placement and Alpha HB score was 0.709, while the EF 1% value was 61.74. An AUC value of 0.5 corresponds to a random ranking, while a value of 1.0 represents a perfect score (all actives ranked above the decoys) [20,27]. The ROC curve represents sensitivity (proportion of true positives) as a function of specificity (proportion of false positives). Therefore, the area under the curve (AUC) value provides an objective measure of a classifier's overall performance, where a value of 0.709 indicates a 70.9 % accuracy [28].

A lower docking number indicates a more favorable position in the receptor-binding site [29]. The molecular docking of thirteen hit molecules and the uPA protein involves ligand conformation as well as orientation (or posing) within a targeted binding site and comprises two main steps: prediction of multiple structural conformations in a binding pocket (pose) and scoring the pose to rank multiple solutions [30]. Subsequently, the chemical substances from the docking result are classified as flavonoids with anticancer activities [31].

Based on the docking score, the four hit molecules isorhamnetin, rhamnetin, quercetin, and kaempferol had the best docking scores compared to the others (-129.64; -128.37; -120.98; -116,84 kcal/mol). Isorhamnetin and rhamnetin had higher docking scores than that of doxorubicin as positive control (-123.81 kcal/mol). These two compounds are metabolites of quercetin and naturally occurring O-methylated flavonol. The methylation reaction increases the metabolic stability of flavonoids that have better bioavailability. This leads to better absorption and increases permeability across membranes [32]. Quercetin has been found to inhibit serine proteases (uPA) with an IC50 value of 7 μM [33].

The chemical structure of the four molecules was constructed by two benzene rings (A and B) as an aromatic ring and a hydrophobic region connected by a heterocyclic pyran ring (C) consisting of oxygen atoms as a metal ligator scaffold, as shown at Figure 3 [34].

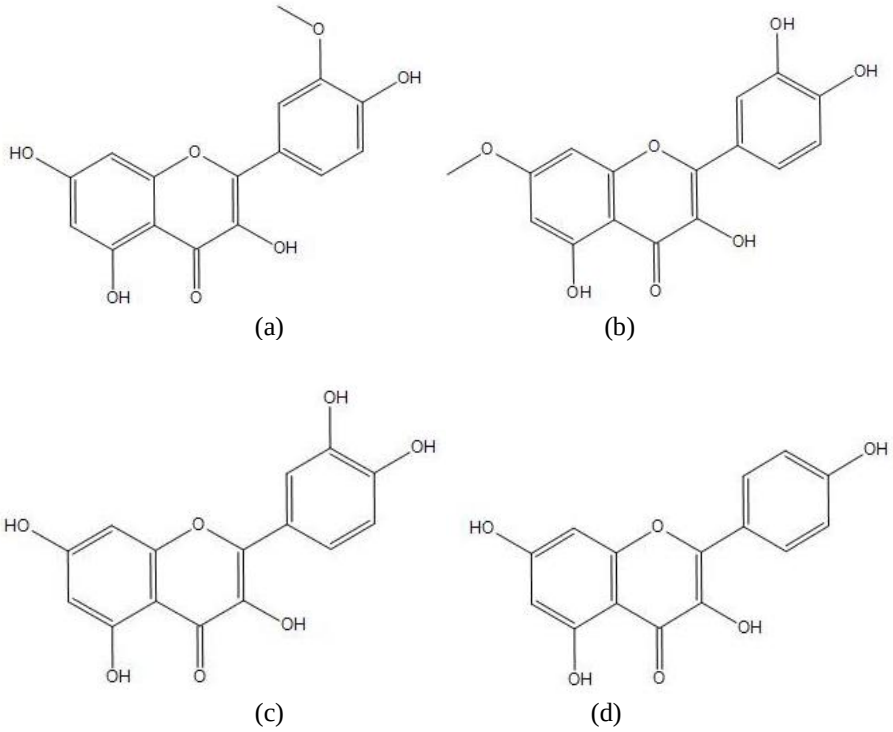

Figure 3 2D structure of the four best-docked flavonoids: (a) isorhamnetin; (b) rhamnetin; (c) quercetin; (d) kaempferol. The ligands were built using the MOE software.

The ligands have interaction of hydrogen bonds with Asp189, Ser190, Ser195, and Gly219. The ligand-Ser195 complex is located at the surface-exposed reactive center loop (RCL) of the SPD of uPA [3]. The hydrogen bond in Ser190 makes an additional bond at the S1 site by interaction with the hydroxyl side chain, which can provide increased affinity as an inhibitor. Isorhamnetin, quercetin, and kaempferol interact with Asp189. The side chain hydroxyl group in flavonoid as an inhibitor makes two hydrogen bonds, with the carboxylate of Asp189 and the carbonyl oxygen of Gly219 [22]. Isorhamnetin forms hydrogen interaction with Asp189 and Gly219, while rhamnetin has no interaction with Asp189. These differences make the inhibitor potency of isorhamnetin stronger than that of rhamnetin. Kaempferol had the highest docking score, because it has one hydroxyl group in the B ring.

The MD simulation is commonly applied to search the optimal structure of the initial structure under the current conditions. The RMSD profile takes as reference the first frame of the simulation, which is superimposed onto the rest of the frames. The RMSD values (i.e. the structural differences with respect to the reference frame) increased over the simulation time until the system reached a stable conformation [35]. The average RMSD value of the backbone atoms in isorhamnetin was 0.197, showing the smallest RMSD, i.e. greater stability, during the entire MD simulation. The increasing RMSD value indicates that the structure of the macromolecule enzymes started to open (unfold) and the ligand would look for the corresponding binding site or appropriate coordinate of the protein [36]. All fluctuations of the RMSD values of all ligands were under 3Å, which can be stated as stable conformation during the 100 ns of simulation (Figure 4).

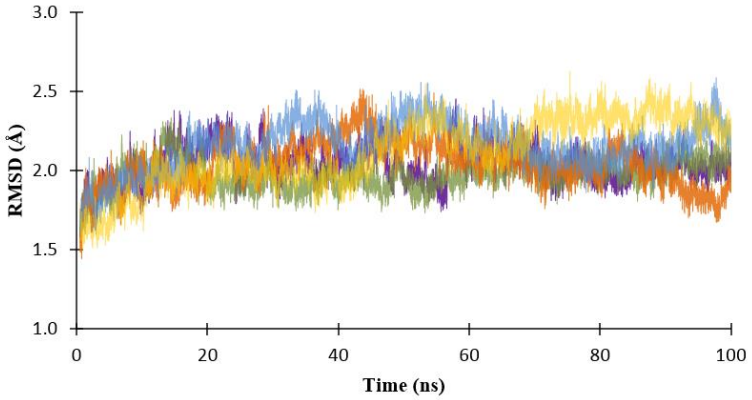

Figure 4 The backbone RMSD of the main protein atoms of each ligand for isorhamnetin, rhamnetin, quercetin, kaempferol, and doxorubicin, colored green, yellow, blue, orange, and purple, respectively.

The RMSF value is the measure of the deviation between the atomic positions of each protein residue, indicating the difference between the fluctuations in the movement of each residue during the simulation. RMSF profiles are often employed to describe and compare the relative mobility of specific regions of the receptor. The higher RMSF values correspond to flexible loops, while their lower counterparts belong to transmembrane helices, where residues are stabilized by the secondary structure [37]. In the uPA-kaempferol complex, the Ser195 residues showed lower RMSF (0.50 Å) than the rhamnetin complex (0.52 Å), and the quercetin complex (0.55 Å). In the residues of 189 and 190, the doxorubicin and isorhamnetin complexes showed higher RMSF values, i.e. 0.69 and 0.56 Å respectively. This shows that the residue of Ser195 is stabilized by the secondary structure (Figure 5).

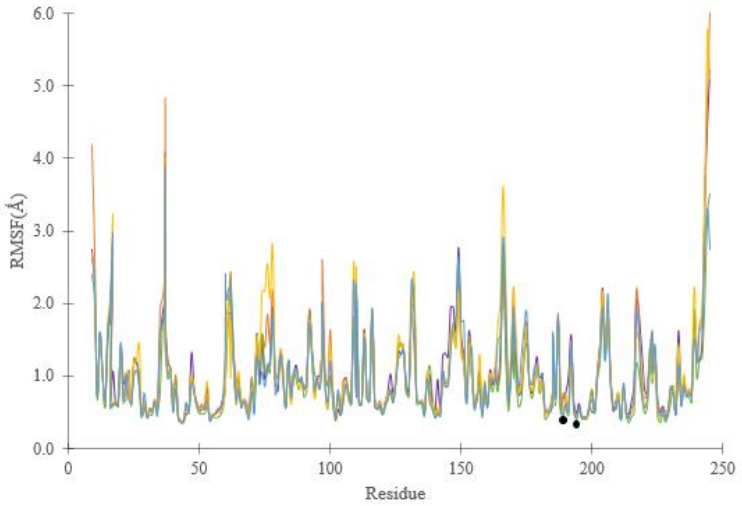

Figure 5 Plot of RMSF residues during MD simulation for isorhamnetin, rhamnetin, quercetin, and kaempferol, indicated by green, yellow, blue, orange, and purple colors, respectively.

3.4 Hydrogen Bond Interaction

Hydrogen bond interactions play an essential role in preserving the secondary structures of protein [38]. For the ligand-uPA complexes in the MD simulation, the amino acid residues Tyr94, His99, Ser190, Gly216, Gly219 showed a hydrogen bond with the ligand. The MD simulation started from docking poses with similar orientations. The results demonstrated that the amino acid residue Ser190 is a crucial residue for uPA activity. The binding complex of isorhamnetin as observed in uPA involves H-bond interaction with the key residue of Ser190 with a distance of 2.43 Å (strong hydrogen bond). In the formation of a hydrogen bond, the distance between the H and the acceptor (A) atoms must be smaller compared to the sum of their corresponding van der Waals radii [39]. The binding conformations of the final snapshot of rhamnetin, quercetin, kaempferol, and doxorubicin in the MD simulation revealed different H-bond interactions from the docking results (Figure 6). The difference from the MD simulation is that the transitions between folded and unfolded states can be obtained.

The hydrogen bond occupancy is depicted in Table 1. Rhamnetin with a total of 54 hydrogen bonds had the highest occupancy at 38.24%, where the hydrogen bond interacted with GLY219. A hydrogen occupancy of 27.45% was observed, where kaempferol plays a role as donor to Asp189, and 13.73% with Ser190, and it has a total of 53 hydrogen bonds. The total hydrogen bond and hydrogen bond occupancy determine the stability of the complex. Meanwhile isorhamnetin and

quercetin had occupancy less than 10%, and doxorubicin had no hydrogen bond occupancy.

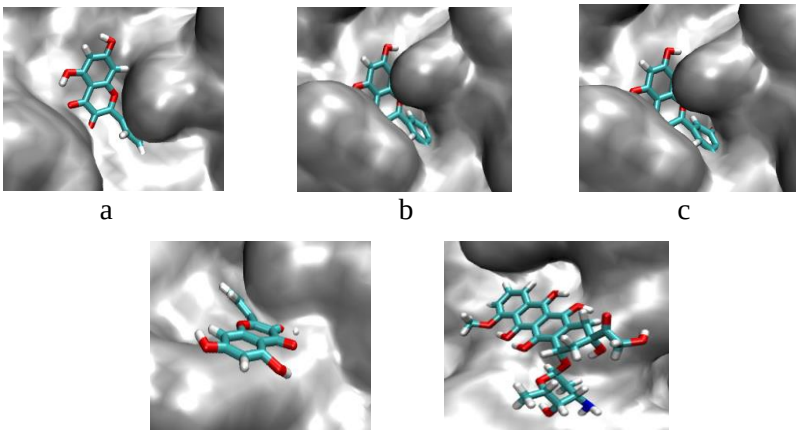

Figure 6 The ligand-protein complexes in the Molecular Dynamics (MD) simulations at the final snapshots (100 ns). The ligands: isorhamnetin (a), rhamnetin (b), quercetin (c), kaempferol (d), and doxorubicin (e) are represented as sticks and the protein as wires.

Table 1 The hydrogen bond occupancy.

Ligand	Donor	Acceptor	Occupancy (%)
Rhamnetin	RHA246-Side	Gly219-Main	38.24
Kaempferol	KAE246-Side	Asp189-Side	27.45
	Ser190-Side	KAE246-Side	13.73

3.5 MM-PBSA

Once the optimal conformation is reached, a balanced conformation is maintained, which is useful for the conformational selection of the MM-PBSA calculation of uPA's binding free energy with all the compounds. The negative value of the ΔG_{bind} at 310 K shows the energetically favorable binding affinity of the ligand to the protein [40]. In addition, the cumulative negative contribution of the van der Waals, electrostatic as well as non-polar solvation energy interaction with the uPA-complexes' stability. Quercetin had a lower negative binding energy compared to isorhamnetin, rhamnetin as well as kaempferol and is therefore a promising agent modification for uPA inhibitors. The binding energy of uPA-rhamnetin was predicted as a substantial energy contribution with ΔG_{bind} of -59.21 kcal/mol (Table 2).

Table 2 MM-PBSA free binding energy of uPA complexes.

Compound	ΔE_{vdw} (kJ/mol)	ΔE_{ele} (kJ/mol)	ΔG_{PB} (kJ/mol)	ΔG_{NP} (kJ/mol)	ΔG_{bind} (kJ/mol)
Isorhamnetin	−154.81±0.14	−27.20±0,18	142.52±0.10	−14.61±0.00	−54.11±0.06
Rhamnetin	−155.32±0.29	−40.16±0.13	150.56±0.38	−14.43±0.02	−59.35±0.20
Quercetin	−136.08±0.10	−47.34±0.21	149.36±0.53	−13.36±0.03	−47.41±0.20
Kaempferol	−138.97±0.51	−49.65±0.91	143.10±1.17	−13.12±0.03	−58.63±0.28
Doxorubicin	−118.43±0.08	−27.68±0.18	97.37±0.66	−12.06±0.03	−60.80±0.38

4 Conclusion

Structure-based pharmacophore modeling and virtual screening successfully identified several flavonols as new inhibitors of uPA. Four flavonols (quercetin, isorhamnetin, rhamnetin, and kaempferol) indicated good affinity, i.e. equal to that of doxorubicin, a known uPA inhibitor. Some important residues, known to play the role of serin protease, i.e. Asp189, Ser195, and Gly219, were visualized. The MD simulations proved that the complex between uPA-rhamnetin is the stablest and the hydrogen bonds involved in the ligand-protein interaction confirmed those of the molecular docking. Several hydrophobic interactions with Gln192 residue were also detected, which is predicted could stabilize the complex. This study adds more insight to the discovery of a novel plant-based uPA inhibitor. However, *in-vitro* and *in-vivo* studies are still required to further propose rhamnetin as uPA inhibitor.

Acknowledgements

The authors would like to thank the Directorate General of Higher Education, Ministry of National Education, Indonesia for financial support through PDD Grant 2018. The authors also thank Prof. Dr. apt. Arry Yanuar, M.Si., who prepares the three-dimensional structural database of chemical compounds from the ligand structure of Indonesian natural products.

References

[1] Tang, L., Han. X., *The Urokinase Plasminogen Activator System in Breast Cancer Invasion and Metastasis*, Biomedicine and Pharmacotherapy, **67**(2), pp. 179-182, 2013. DOI:10.1016/j.biopha.2012.10.003.

[2] Al-Sha'er, M. A., Khanfar, M.A., Taha, M. O., *Discovery of Novel Urokinase Plasminogen Activator (uPA) Inhibitors Using Ligand-based Modeling and Virtual Screening Followed by In vitro Analysis*, Journal of Molecular Modelling, **20**(1), pp. 1-15, 2014. DOI:10.1007/s00894-014-2080-4.

[3] Skeldal, S., Larsen, J.V., Pedersen, K.E., Petersen, H.H., Egelund, R., Christensen, A., Jensen, J.K., Gliemann, J., Andreasen, P.A., *Binding Areas of Urokinase-type Plasminogen Activator-plasminogen Activator Inhibitor-1 Complex for Endocytosis Receptors of the Low-density Lipoprotein Receptor Family, Determined by Site-directed Mutagenesis*, The FEBS Journal, **273**, pp. 5143-5159, 2006. DOI:10.1111/j.1742-4658.2006.05511.x.

[4] Sulimov, V.B., Katkova, E.V., Oferkin, I.V., Sulimov, A.V., Romanov, A.N., Roschin, A.I., Beloglazova, I.B., Plekhanova, O.S., Tkachuk, V.A., Sadovnichiy, V.A., *Application of Molecular Modeling to Urokinase Inhibitors Development*, Biomed Research International, pp. 1-15, 2014, DOI:10.1155/2014/625176.

[5] Nisar, B., Sultan, A., Rubab, L., *Comparison of Medicinally Important Natural Products Versus Synthetic Drugs-A Short Commentary*, Natural Products Chemistry & Research, **6**(2), pp. 1-2, 2017. DOI:10.4172/2329-6836.1000308.

[6] Mitra, S., Dash, R., *Natural Products for the Management and Prevention of Breast Cancer*, Evidence-based Complementary and Alternative Medicine, pp. 1-17, 2018. DOI:10.1155/2018/8324696.

[7] Xiao, J., *Dietary Flavonoid Aglycones and Their Glycosides: Which Show Better Biological Significance*, Critical Reviews in Food Science and Nutrition, **57**(9), pp. 1874-1905, 2017. DOI:10.1080/10408398.2015.1032400.

[8] Yanuar, A., Mun'im, A., Lagho, A.B.A., Syahdi, R.R., Rahmat, M., and Suhartanto, H., *Medicinal Plants Database and Three-dimensional Structure of the Chemical Compounds from Medicinal Plants in Indonesia*, International Journal of Computer Science Issues, **8**(5), pp. 180-183, 2011.

[9] Salentin, S., Schreiber, S., Haupt, V.J., Adasme, M.F., Schroeder, M., *PLIP: Fully Automated Protein-ligand Interaction Profiler*, Nucleic Acids Research Advance, **43**, pp. 1-5, 2015. DOI:10.1093/nar/gkv315.

[10] Edwardson, D.W., Narendrula, R., Chewchuk, S., Mispel-Beyer, K., Mapletoft, J.P.J., Parissenti., A.M., *Role of Drug Metabolism in the Cytotoxicity and Clinical Efficacy of Anthracyclines*, Current Drug Metabolism, **16**(6), pp. 412-426, 2015. DOI:10.2174/1389200216888150915112039.

[11] Schuliga, M., *The Inflammatory Actions of Coagulant and Fibrinolytic Proteases in Disease*, Mediators of Inflammation, pp. 1-9, 2015:437695. DOI:10.1155/2015/437695.

[12] Agarwal, R., Shrestha, U.R., Chu, X-D., Petridis, L., Smith, J.C., *Mesophilic Pyrophosphatase Function at high Temperature: A Molecular dynamics Simulation Study*, Biophysical Society, **119**(1), pp. 142-150, 2020. DOI:10.1016/j.bpj.2020.05.021.

[13] Genheden, S., Ryde, U., *The MM/PBSA and MM/GBSA Methods to estimate Ligand-binding Affinities*, Expert Opinion on Drug Discovery, **10**(5), pp. 449-61, 2015. DOI:10.1517/17460441.2015.1032936.

[14] Zhu, M., Gokhale, V.M., Szabo, L., Munoz, R.M., Baek, H., Bashyam, S., Hurley, L.H., Von Hoff, D.D., Han, H., *Identification of a novel Inhibitor of Urokinase-type Plasminogen Activator*, Molecular Cancer Therapeutics, **6**(4), pp. 1348-1354, 2007. DOI: 10.1158/1535-7163.MCT-06-0520.

[15] Kumar, G., Banerjee, T., Kapoor, N., Surolia, N., Surolia, A., *SAR and pharmacophore Models for the rhodanine Inhibitors of Plasmodium falciparum Enoyl-acyl carrier Protein Reductase*, IUBMB Life, **62**(3), pp. 204-213, 2010. DOI:10.1002/iub.306.

[16] Sunseri, J., Koes, D.R., *Pharmit: interactive Exploration of chemical Space*, Nucleic Acids Research, **44**, pp. 442-448, 2016. DOI:10.1093/nar/gkw287.

[17] Fernandes, T.B., Segretti, M.C.F., Polli, M.C., Parise-Filho, R., *Analysis of the applicability and Use of Lipinski`s Rule for central Nervous System Drugs*, Lett. Drug Des. Discov., **13**(10), pp. 999-1006, 2016. DOI: 10.2174/1570180813666160622092839.

[18] Fei, J., Zhou, L., Liu, T., Tang, X.Y., *Pharmacophore modeling, Virtual Screening, and molecular Docking Studies for Discovery of Novel Akt2 Inhibitors*, International Journal Medical Sciences, **10** (3), pp. 265-274, 2013. DOI:10.7150/ijms.5344.

[19] Mysinger, M.M., Carchia, M., Irwin, J.J., Shoichet, B.K., *Directory of useful Decoys, Enhanced (DUD-E): Better Ligands and Decoys for Better Benchmarking*, Journal Med. Chem., **55**(14), pp. 6582-6594, 2012. DOI: 10.1021/jm300687e.

[20] Empereur-Mot, C., Zagury, J.F., Montes, M., *Screening Explorer - An interactive Tool for the Analysis of Screening Results*, J. Chem. Inf. Model., **56**(12), pp. 2281-2286, 2016. DOI:10.1021/acs.jcim.6b00283.

[21] Wang, C., Greene, D., Xiao, L., Qi, R., Luo, R., *Recent Developments and Applications of the MMPBSA Method*, Front. Mol. Biosci., **4**, pp. 1-18, 2018. DOI: 10.3389/fmolb.2017.00087.

[22] Katz, B.A., Mackman, R., Luong, C., Radika, K., Martelli, A., Sprengeler, P.A., Wang, J., Chan, H., Wong, L.., *Structural Basis for Selectivity of a small Molecule, S1-binding, Submicromolar Inhibitor of Urokinase-type plasminogen Activator*, Chemistry Biology, **7** (4), pp. 299-312, 2000. DOI:10.1016/S1074-5521(00)00104-6.

[23] Chen, C., Wang, T., Wu, F., Huang, W., He, G., Ouyang, L., Xiang, M., Peng, C., Jiang, Q., *Combining Structure-based pharmacophore Modeling, virtual Screening, and In Silico ADMET Analysis to discover Novel Tetrahydro-quinoline based Pyruvate Kinase Isozyme M2 Activators with*

antitumor Activity, Drug Design Development Therapy, **8**, pp. 1195-1210, 2014. DOI:10.2147/DDDT.S62921.

[24] Kalyaanamoorthy, S., Chen, Y.P.P., *Structure-based Drug Design to Augment Hit Discovery*, Drug Discovery Today, **16**(17/18), PP. 831-839, 2011. DOI: 10.1016/j.drudis.2011.07.006.

[25] Koes, D.R., Camacho, C.J., *Shape-based Virtual Screening with Volumetric Aligned Molecular Shapes*, Journal of Computational Chemistry, **35**(25), pp. 1821-1834, 2014. DOI: 10.1002/jcc.23690.

[26] Rao, S.N., Head, M.S., Kulkarni, A., LaLonde, J.M., *Validation studies of the Site-directed Docking Program LibDock*, Journal Chemistry Inf. Model, **47**(6), pp. 2159-2171, 2007. DOI: 10.1021/ci6004299.

[27] Vogel, S.M., Bauer, M.R., Boeckler, F.M., *DEKOIS: Demanding Evaluation Kits for Objective In Silico Screening - A Versatile Tool for Benchmarking Docking Programs and Scoring Functions*, Journal Chemistry Inf. Model, **51**(10), pp. 2650-2665, 2011. DOI:10.1021/ci2001549.

[28] Fawcett, T., *An Introduction to ROC analysis*, Pattern Recognit. Lett., **27**(8), pp. 861-874, 2005. DOI:10.1016/j.patrec.2005.10.010.

[29] Guedes, I.A., de Magalhães, C.S., Dardenne, L.E., *Receptor-ligand Molecular Docking*, Biophys. Rev., **6**(1), pp. 75-87, 2014. DOI:10.1007/s12551-013-0130-2.

[30] Meng, M., Zhang, X., Mezei, M., & Cui, M., *Molecular Docking: a powerful Approach for Structure-based Drug Discovery*, Curr. Comput. Aided Drug Des., **7**(2), pp. 146-157, 2011.

[31] Weston, L.A., Mathesius, U., *Flavonoids: Their Structure, Biosynthesis and Role in the Rhizosphere, Including Allelopathy*, Journal Chemical Ecology, **39**(2), pp. 283-297, 2013. DOI: 10.1007/s10886-013-0248-5.

[32] Kandakumar, S., Manju, D.V., *Pharmacological Applications of Isorhamnetin: A Short Review*, International Journal Trend Sciences Research Development, **1**(4), pp. 672-678, 2017. DOI:10.31142/ijtsrd2202.

[33] Xue, G., Gong, L. Yuan, C. Xu, M., Wang, X., Juang, L., Huang, M., *A Structural Mechanism of Flavonoids in Inhibiting Serine Proteases*, Food and Function, **8**(7), pp. 2437-2443, 2017. DOI:10.1039/c6fo01825d.

[34] Kumar, S., Pandey, A. K., *Chemistry and Biological Activities of Flavonoids: An Overview*, The Scientific World Journal, **2013**, pp. 1-16, 2013. DOI:10.1155/2013/162750.

[35] Kitchen, D. B., Decornez, H., Furr, J. R., Bajorath, J., *Docking and Scoring in Virtual Screening for Drug Discovery: Methods fad Applications*, Nature Reviews Drug Discovery, **3**(11), pp. 935-947, 2004. DOI:10.1038/nrd1549.

[36] Torrens-Fontanals, M., Stepniewski, T. M., Aranda-García, D., Morales-Pastor, A., Medel-Lacruz, B., Selent, J., *How Do Molecular Dynamics Data Complement Static Structural Data of GPCRs*, International Journal of Molecular Sciences, **21**(16), pp. 5933, 2020. DOI:10.3390/ijms21165933.

[37] Setiawan, M. T., Yanuar, A., *Virtual Screening and Molecular Dynamics Simulation of Compounds from the Herbal Database of Indonesia Against Histone Deacetylase 2*, International Journal of Applied Pharmaceutics, **10**(1), pp. 235-239, 2018. DOI:10.22159/ijap.2018.v10s1.52.

[38] Yanuar, A., Chavarina, K. K., Syahdi, R. R., *Molecular Dynamic Simulation Analysis on Marine Fungi Compounds Against EGFR and VEGFR-2 Inhibitory Activity in Non-small Cell Lung Cancer*, Journal of Young Pharmacists, **10**(2), 2018. DOI:10.5530/jyp.2018.2s.6.

[39] Gao, Y., Mei, Y., Zhang, J. Z. H., *Treatment of Hydrogen Bonds in Protein Simulations*, in Advanced Materials for Renewable Hydrogen Production, Storage and Utilization, 2015. DOI:10.5772/61049.

[40] Kumari, R., Kumar, R., Open-Source Drug Discovery Consortium, Lynn, A., *g _ mmpbsa - A GROMACS Tool for MM-PBSA and Its Optimization for High-throughput Binding Energy Calculations*, Journal of Chemical Information and Modeling, **54**, pp. 1951-1962, 2014. DOI:10.1021/ci500020m